Resonance Raman Intensities Demonstrate that C5 Substituents Affect the Initial Excited-state Structural Dynamics of Uracil more than C6 Substituents.

*Faranak Teimoory and Glen R. Loppnow**

Department of Chemistry, University of Alberta, Edmonton, AB CANADA T6G 2G2

Mad about U: The initial excited-state structural dynamics of C5 and C6 uracil derivatives derived from absorption and UV resonance Raman spectroscopy are compared. By calculating the reorganization energies on an internal coordinate basis, a clearer understanding of the role of the C5 and C6 substituents on the initial excited-state structural dynamics and the resulting photochemistry emerges.

Keywords: spectroscopy, nucleobases, DNA, initial excited-state structural dynamics, uracil, thymine, 6-deuterouracil, 6-methyluracil, 5,6-dideuterouracil.

Abstract

Resonance Raman-derived initial excited-state structural dynamics provide insight into the photochemical mechanisms of pyrimidine nucleobases, in which the photochemistry appears to be dictated by the C5 and C6 substituents. The absorption and resonance Raman spectra and excitation profiles of 5,6-dideuterouracil (5,6-d_2-U) are measured here to further test this photochemical dependence on C5 and C6 substituents. The resulting set of excited-state reorganization energies of the observed internal coordinates are calculated and compared to those of other 5- and 6-substituted uracils. The results show that the initial excited-state dynamics along the C5C6 stretch responds to changes in mass at C5 and C6 in the same manner, but that the in-plane bends at C5 and C6 are more sensitive to substituents at the C5 position than at C6. In addition, the presence of two

deuterium substituents on C5 and C6 decreases the initial excited-state structural dynamics along these in-plane bends, in contrast to what is observed in the presence of two CH_3 groups on C5 and C6. The results are discussed in the context of DNA nucleobase photochemistry.

Introduction

Nucleobase photochemistry is the initial step in the complex chain of events that results in UV-induced DNA damage, and ultimately carcinogenesis [1]. Nucleic acid photochemistry is primarily localized in the pyrimidine nucleobases, thymine and uracil, which have a very similar structure. They differ only in their C5 substituents, which is H in uracil and CH_3 in thymine. However, the photoproducts and their yields for uracil and thymine are different (Chart 1). Thymine yields the cyclobutyl photodimer (CPD) and uracil yields the photohydrate as the major photoproducts, respectively, of UVC irradiation. It seems that C5 and C6 substituents may play a significant role in the initial excited-state structural dynamics and resulting photochemistry [2].

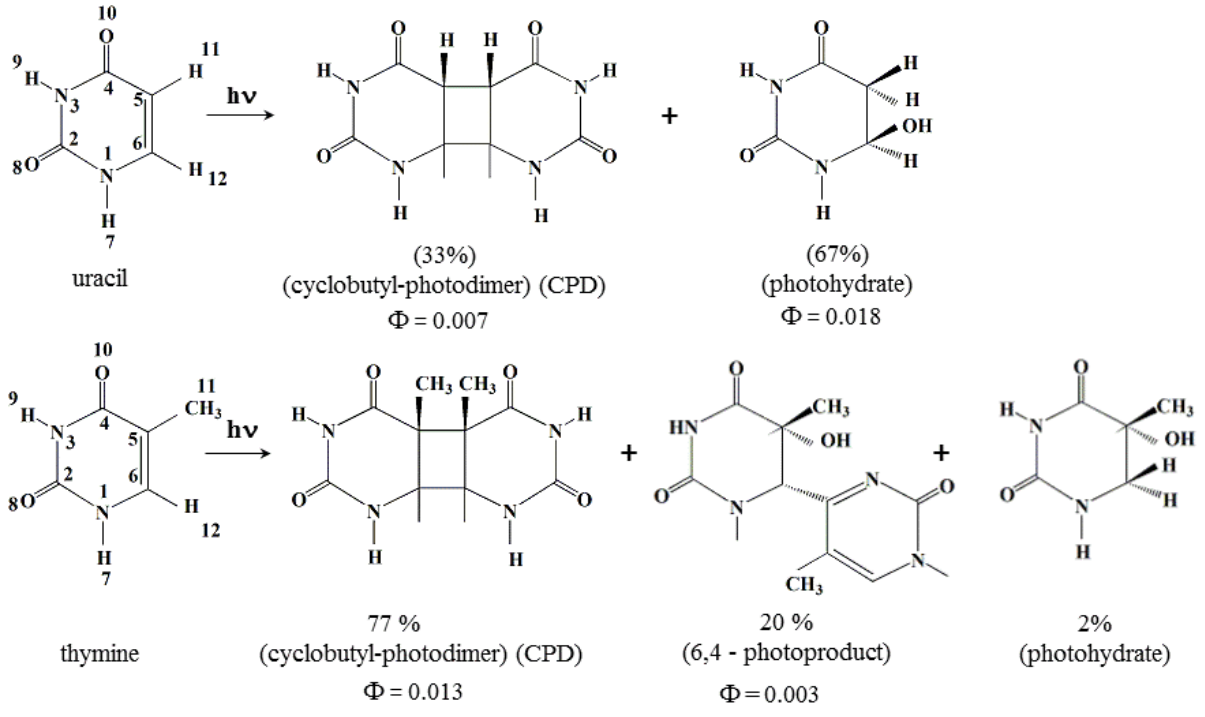

Scheme 1. Photochemistry of uracil and thymine [2].

Many studies of the *electronic* excited-state dynamics have been performed, both theoretically and experimentally [3-6]. Fluorescence lifetime studies and femtosecond transient absorption spectroscopy report very short excited singletstate lifetimes of <100 and 540 fs for uracil and thymine [4,7], respectively, which result from ultrafast internal conversion [5,6]. Thymine and all the C5-substituted uracil derivatives exhibit longer excited-state lifetimes and biexponential fluorescence decays [4]. Also, the S_0/S_1 conical intersection is predicted to be reached on the excited-state surface via pyramidalization and bending motions of the C5 substituents [4]. Therefore, more excited-state *structural* dynamics studies are needed to understand the role of C5 and C6 substituents on the excited-state structural dynamics. The ultrafast excited-state lifetimes of uracil and thymine in the condensed phase [8,9] restrict the probes available for studying the initial excited-state *structural* dynamics.

The initial excited-state structural dynamics of nucleobases with short-lived excited-states can be obtained by using resonance Raman intensities, absorption spectra and a self-consistent time-dependent wavepacket formalism. Such an analysis has been performed on numerous uracil derivatives [10-14] in an attempt to elucidate photochemical mechanisms in DNA components. Previous elucidation of the initial excited-state structural dynamics of C5 and C6 methylated uracil derivatives have shown that methyl substitution increases the initial excited-state structural dynamics along the C5C6 bond lengthening coordinate [10,11,13,14]. Similarly, methyl substitution at C6 shows lower initial excited-state distortional forces along the C5X and C6X in-plane bends than substitution at C5 [13]. We here examine the initial excited-state structural dynamics of 5,6-d_2-U (Scheme 1) using resonance Raman and absorption spectroscopy to further test this model of C5/C6 substituent-dependent initial excited-state structural dynamics.

Experimental

A solution of 5,6-dideuterouracil (5,6-d_2-U, 99%, C/D/N isotopes, Pointe-Claire, Quebec) and 0.3 M lithium sulfate (99%, EMD Chemicals Inc., Gibbstown, NJ) was prepared by dissolving the solid samples in nanopure water obtained from a Barnstead (Boston, MA) water filtration system. The addition of lithium sulfate did not noticeably change the absorption or resonance Raman spectra of 5,6-d_2-U. The UV resonance Raman spectra of solutions containing 1 mM 5,6-d_2-U and 0.3 M lithium sulfate internal standard were obtained at excitation wavelengths of 250, 257, 266 and 275 nm with laser powers of 5-12 mW, as previously described [13,15,16]. Spectral slit widths were 5-7 cm^{-1} and the total accumulation time was 20-30 min for each spectrum. The same solution conditions were used in a UV resonance Raman microscope (Renishaw, Chicago, IL) to obtain the 257 nm resonance Raman spectrum in the overtone and combination band region with a laser power of 5-8 mW [11].

Absorption spectra (Hewlett-Packard, model 8452A, Sunnyvale, CA) of the samples were taken before and after each Raman spectrum [13]. A few solvents (cyclohexane, ethanol, N,N-dimethylformamide, acetic acid) with known peak positions were used for frequency calibration with an accuracy of ±5 cm^{-1}. The data were analysed as described previously [13].

The methods used for converting the resonance Raman intensities to differential cross-section have been described previously [10-16]. The experimental resonance Raman differential cross-sections of sulfate used for the calculations were 3.30×10^{-12}, 2.87×10^{-12}, 2.42×10^{-12} and 2.05×10^{-12} $Å^2$ $molecule^{-1}$ sr^{-1} at 250, 257, 266 and 275 nm, respectively [10-13].

The equations [17-20] and their implementation [10-17,19-22], in the analysis of resonance Raman intensities to yield initial excited-state structural dynamics have been described extensively.

All experimentally observed fundamental modes of 5,6-d_2-U were considered in the time-dependent calculation.

Table 1: Harmonic Mode Parameters of 5,6-d_2-U[a]

Mode ν(cm^{-1})	Assignment[b] (PED%)	β/ħ (cm^{-1})
571	Ring def 3 [53], be(C2O8) [-10], ν(N3C4) [-7], ν(C4C5) [6], be(C4O10) [-6]	108
777	be(C5D11) [52], be(C6D12) [31], ν(C5C6) [-6]	178
1191	ν(C2N3) [17], ν(C4C5) [14], be(N1H7) [12], ν(N1C2) [-11], be(C5D11) [-9], ν(C5C6) [-8], be(C6D12) [8], be(C2O8) [6], ν(N1C6) [5]	202
1274	ν(C2N3) [20], ν(N1C2) [-16], ν(C4C5) [-10], be(C4O10) [-9]	369
1403	be(N1H7) [47], ν(N1C6) [24], ν(C2O8) [-10]	168
1593	ν(C5C6) [63], ν(N1C6) [-11], be(C6D12) [6]	382
1661	ν(C4O10) [71], ν(C4C5) [-8], Ring def 2 [5]	448

[a] Normal modes listed here are the experimental wavenumbers of 5,6-d_2-U. The excited-state slopes (β/ħ) were obtained by fitting the excitation profiles and absorption spectra in Figs. 2 and 3 with Equations 1 and 2 in reference 13 using the following parameters: temperature T = 298 K, Brownian oscillator line shape $\kappa = \Lambda/D = 0.1$, Gaussian homogeneous line width Γ_G =1310 cm^{-1}, inhomogeneous line width θ = 1150 cm^{-1}, zero-zero energy E_0 = 37280 cm^{-1}, and transition length M= 0.67 Å. The errors in the parameters are estimated in the calculation as follows: zero-zero energy (E_0), ±1%; transition length (M), ±1%; homogeneous line width (Γ), ±5%; inhomogeneous line width (θ), ±5%; and displacements, ±5%.

[b] A Gaussian09 and GAR2PED computation was used to obtain mode assignments and internal coordinates. Abbreviations: ν, stretch; be, bend; def, deformation. The numbers in square brackets represent the potential energy distributions (PEDs) of the internal coordinate(s) in %. The internal coordinates with PEDs < 5% are not reported. The sign refers to the relative phase of the internal coordinate.

The mode assignments were obtained by a density functional theory (DFT) computation at the B3LYP/6-311G(d,p) level of theory using the default gradients in the Gaussian09 package [23] and

performed on the initial planar Cs structure of uracil to give the minimum energy structure. Both Singh et al. [24] and Khaikin et al. [25] have shown that DFT computations for these uracil-like systems are in great agreement with restricted Hartree-Fock and DFT methods using different basis sets, as well as with experimental IR and Raman spectra. The isotope effect on the uracil frequencies was determined from a single point calculation on the optimized structure, replacing the natural abundance mass of H with the isotopic mass of 2 for deuterium at both C5 and C6. Frequencies were not scaled. The set of non-redundant symmetry coordinates of 5,6-d_2-U was constructed by GAR2PED [26].

Results

The resonance Raman spectra of 5,6-dideuterouracil (5,6-d_2-U) as a function of excitation wavelength are shown in Figure 1 and all the mode assignments and excited-state slopes are described in Table 1. The most intense modes observed in the resonance Raman spectra of 5,6-d_2-U include the 1661 cm^{-1} peak corresponding to the C4O10 stretch, the 1593 cm^{-1} peak corresponding to the C5C6 stretch, the 1274 and 1191 cm^{-1} peaks corresponding to ring stretches, the 777 cm^{-1} peak corresponding to the C5D11 and C6D12 in-plane bends, and the 571 cm^{-1} peak corresponding to a ring deformation. The similar frequencies and similar relative intensities at the different excitation wavelengths indicate that the Raman spectra are resonant with a single, allowed excited state. The spectra exhibit good signal-to-noise quality.

The experimental and simulated absorption spectra of 5,6-d_2-U are shown in Figure 2, which also shows the excitation wavelengths used for measuring the resonance Raman spectra. Deviations between the experimental and calculated absorption spectra (Figure 2) at wavenumbers greater than 38,000 cm^{-1} are due to transitions to higher electronic excited states that were not considered in this

model (vide infra).

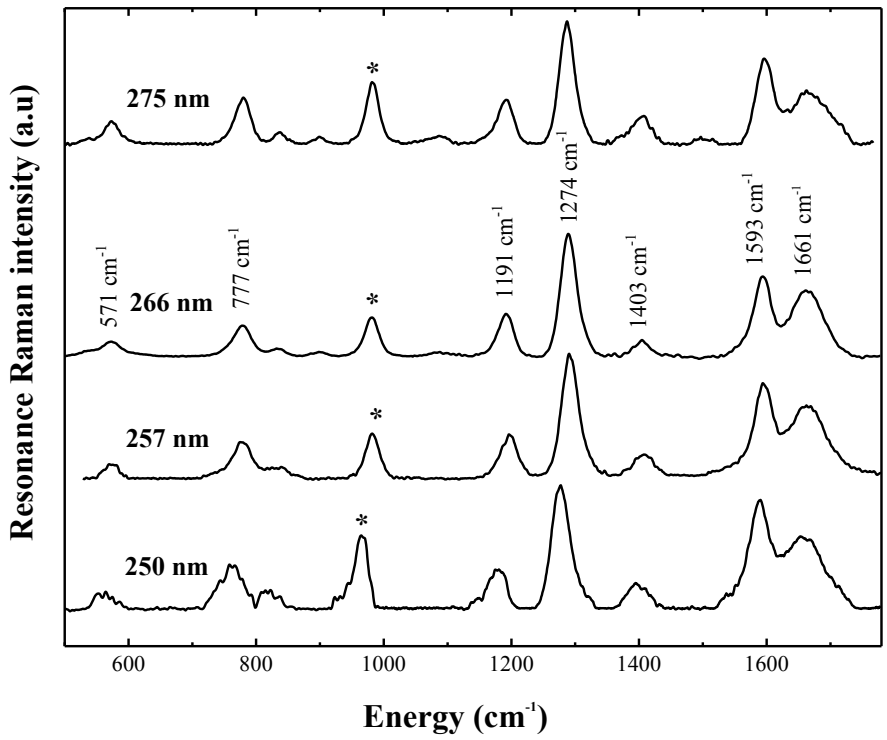

Figure 1. Resonance Raman spectra of 1 mM solutions of 5,6-d_2-U containing 0.3 M lithium sulfate as an internal standard at excitation wavelengths throughout its ~ 260 nm absorption band. Asterisks (*) indicate the internal standard bands. The spectra all have been scaled by the most intense peak and offset along the y axis for clarity.

Figure 3 shows the experimental and simulated resonance Raman excitation profiles. The resonance Raman excitation profiles in Figure 3 clearly reproduce the relative intensities observed in the resonance Raman spectra in Figure 1; the most intense modes in Figure 1 lead to the largest excitation profiles. The experimental cross-sections are reproduced well by the simulated excitation profile.

The overtones and combination bands between 1700 and 3000 cm^{-1} were obtained by the UV resonance Raman microscope at an excitation wavelength of 257 nm and the results are shown in

Table 2. The overtone and combination band intensities are more sensitive to the excited-state parameters than the fundamental resonance Raman intensities. By demonstrating that the fundamental vibration excited-state parameters (Table 1) also reproduce the overtone and combination band intensities as for the fundamental vibrations, the robustness of the excited-state parameters is confirmed. The observed errors between the observed and simulated overtone and combination band cross-sections are within experimental error and are attributed to the high

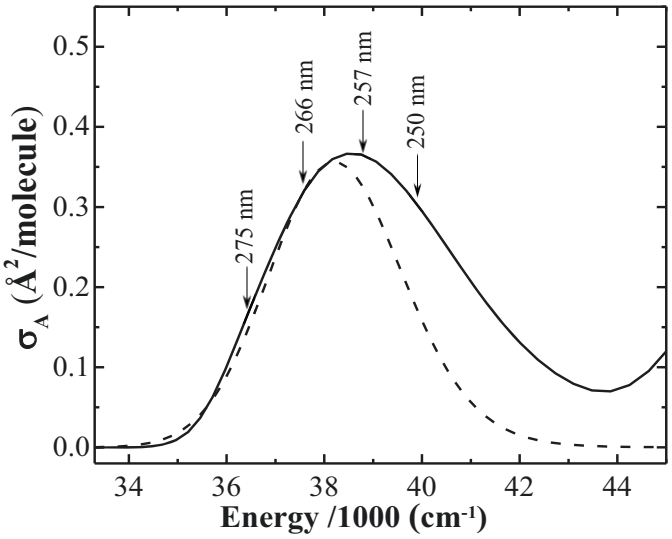

Figure 2. Experimental (solid line) and simulated (dashed line) absorption spectra of 5,6-d_2-U. The simulated absorption spectrum was obtained by using the parameters in Table 1 in Equation 1 of reference 13.

dependence of the peak intensities on the focusing point in the Raman microscope. For the 2337 cm^{-1} overtone/combination band, the most likely source of error is other overtones and combinations in this band that were not included in the model, as this is the only band we were unable to successfully model. We therefore believe the harmonic parameter set is accurate.

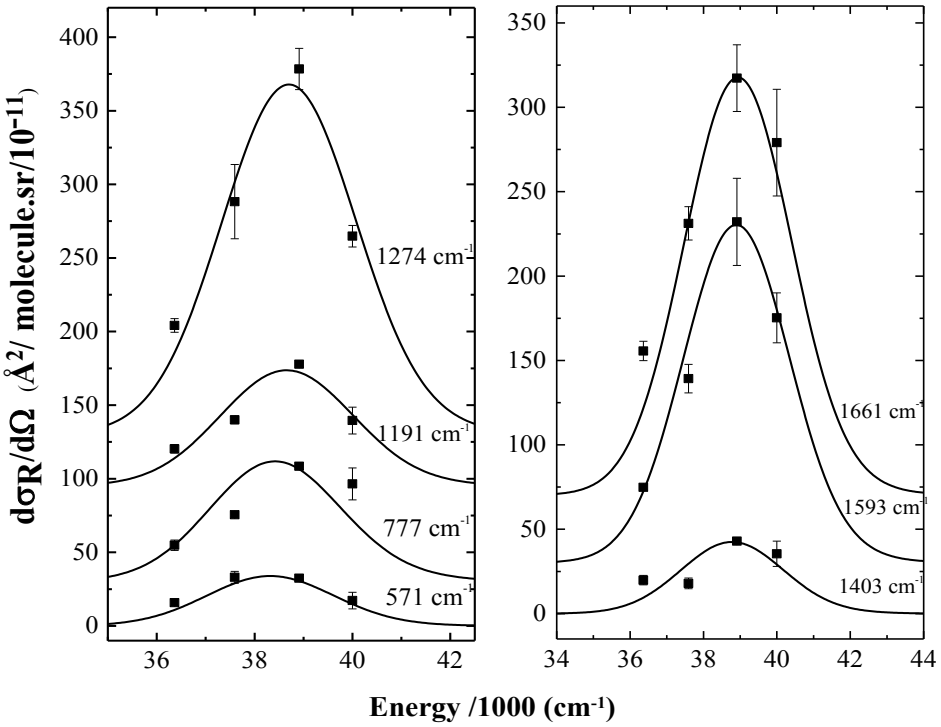

Figure 3. Calculated (solid line) and experimental (points) resonance Raman excitation profiles of 5,6-d_2-U. The excitation profiles were calculated with Equation 2 of reference 13 by using the parameters in Table 1. For greater clarity of presentation, the excitation profiles have been offset along the y axis.

Table 2: Experimental and Calculated Absolute Resonance Raman Overtone and Combination Band Cross-sections of and 5, 6-d_2-U[a]

Mode (cm^{-1})	Mode assignment	$d\sigma_{experimental}/d\Omega$ ($Å^2$/molecule × 10^{10})	$d\sigma_{calculated}/d\Omega$ ($Å^2$/molecule × 10^{10})
2081	1273 + 777	0.41 ± 0.37	0.49
2337	(1593 + 777) + (1191 * 2)	0.92 ± 0.13	0.41
2480	(1661 + 777) + (1191 + 1273)	0.72 ± 0.17	0.85
2589	(1191 + 1403) + (1273 * 2)	0.63 ± 0.11	0.74

[a]Excitation wavelength was 257 nm. Cross-sections were calculated using Equation 2 of reference 13 with the parameters in Table 1.

To understand the role of substituent numbers and position on the resonance Raman spectra and subsequent initial excited-state structural dynamics of uracil, we have compared the spectra of all C5- and C6- methylated and deuterated derivatives in Figure 4 [10-14]. The spectra show good signal-to-noise, facilitating comparisons of frequencies and relative intensities. Similar main peaks in the fingerprint region (1000-1660 cm^{-1}) are observed in all the methylated and deuterated derivatives of uracil, though they differ in frequency, relative peak intensity and mode assignment.

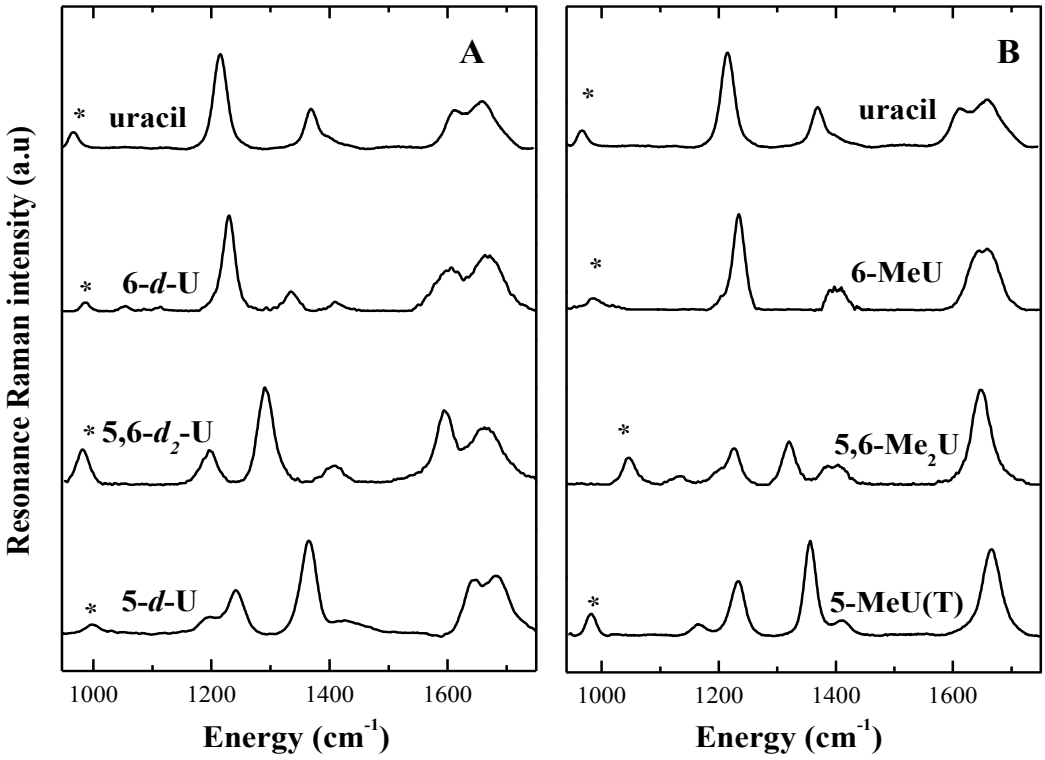

Figure 4. Resonance Raman spectra of aqueous solution of (A) uracil [11], 5-*d*-U [12], 5,6-d_2-U and 6-*d*-U [13], and (B) uracil [11], 5-MeU (T) [10], 5,6-Me_2U [14], and 6-MeU [13] excited at 275 nm. The asterisks (*) indicate the sulfate internal standard peak used in all the compounds except 5,6-Me_2U, in which sodium nitrate was used as the internal standard. The spectra have been offset along the y axis for clarity. Intensities have been normalized to the most intense peak in each spectrum.

The spectral properties, such as the relative intensities, number of peaks and peak frequencies, of all the uracil derivatives exhibits a gradual change as the number and/or position of substituents change. As observed in Figure 4, the comparison of resonance Raman spectra of the deuterated uracil derivatives shows that the spectrum of 5,6-d_2-U is a combination of 5-*d*-U and 6-*d*-U in the range 1200-1400 cm^{-1}. This range corresponds to the C5X and C6X bending coordinates. However, more similarity is generally observed in this spectral region between the spectra of 5-*d*-U and 5,6-d_2-U than between those of 5-*d*-U and 6-*d*-U and between those of 5,6-d_2-U and 6-*d*-U. Similar behavior is observed among the methylated derivatives in the same region. This result shows that the C5 substituent is more significant in affecting the resonance Raman spectra, and subsequent initial excited-state structural dynamics, of uracil derivatives.

The 1600 and 1660 cm^{-1} peaks correspond to the C5C6 and C4O10 stretches, respectively (Table 1). For the deuterated uracil derivatives in Figure 4A, no significant trend with substitution is observed among these modes, although small changes in relative intensities and frequencies are observed. However, much larger changes are seen in these peaks for the methylated uracil derivatives. Methylation at either C5 or C6 causes the two stretches to occur closer in frequency, with only a single peak observed in 5,6-Me_2U and 5-MeU. Vibrational spectra of the isotopic derivatives of 5-MeU (thymine) [27,28] show that the ca. 1630 cm^{-1} peak is composed of only the C5C6 stretch; the C4O10 stretch has lost all intensity. This result shows the importance of C5, more than C6, substituents on the initial excited-state structural dynamics.

Discussion

Each normal mode is constructed of a few internal coordinates (Table 1), including the photochemically active coordinates, such as the C5C6 stretch and C5X and C6X bends, and the non-photochemical internal coordinates, such as the C4O10 stretch and the ring breathing modes.

However, the internal coordinates mix differently in the normal modes dependent on the uracil analogue being examined. Therefore, it is more appropriate to discuss the structural dynamics from the internal coordinate perspective [13,14], rather than the normal modes, to facilitate the comparison between different uracil analogues and identify trends in their initial excited-state structural dynamics.

The reorganization energy (E) along each internal coordinate from electron transfer theory [20,29] is a useful quantitative measure to compare initial excited-state structural dynamics among the different uracil analogues. The percent reorganization energy of each internal coordinate can be obtained from the excited-state slope (β/ħ) along each normal mode, ground-state wavenumber (ῡ), and that internal coordinate's contribution to normal mode (c_{ij}) by Eq. 1:

$$\%\ \text{reorganization energy} = \frac{\sum_{j=1}^{n}\left\{\left(\frac{\left(\frac{\beta}{\hbar}\right)^2}{2\bar{\upsilon}}\right)_j C_{ij}\right\}}{\sum_{j=1}^{n}\left(\frac{\left(\frac{\beta}{\hbar}\right)^2}{2\bar{\upsilon}}\right)_j} \times 100\% \qquad (1)$$

The reorganization energies of the photochemically active internal coordinates of the uracil derivatives are shown in Table 3. Many interesting trends in the internal coordinates as a function of the uracil derivative become clear. Note that no difference in the ring deformation appears to occur with any substituent. For the C5C6 stretch, Table 3 shows that the reorganization energy increases from 6% in uracil [13] to 12-25% when any substitution occurs at C5 and/or C6. For a single deuterium substitution, the reorganization energy along this coordinate increases to 16% and 12% in 5-*d*-U [13] and 6-*d*-U [13], respectively. Interestingly, the presence of the second deuterium

has no additional effect on the initial excited-state structural dynamics of C5C6 stretch coordinate (14% in 5,6-d_2-U) and its reorganization energy is intermediate between that of 5-*d*-U and 6-*d*-U.

Table 3: Internal Coordinate Reorganization Energies of C5- and C6-Deuterated and Methylated Uracil Derivatives[a]

Compound	C5C6 str.	C5 be.	C6 be.	C5 + C6 be.	active	ring def.	C4O10 str.
Uracil[13]	6	13	9	22	28	5	23
5-*d*-U[13]	16	2	16	18	34	4	21
6-*d*-U[13]	12	13	3	16	28	4	20
5,6-d_2-U	14	6	2	8	22	4	22
5-MeU (T)[13]	24	8	15	23	47	5	2
6-MeU[13]	26	7	3	10	36	5	4
5,6-Me_2U[14]	25	7	6	13	38	4	2

[a]In this Table, all reorganization energies are in percentages (%) and calculated by Eq. 1. "C5C6 str." is the C5C6 stretch, "C5 be." is either the C5H, C5C and C5D bending coordinate depending on derivative, "C6 be." is either the C6H, C6C and C6D bending coordinate depending on derivative, "C5 +C6 be." is the sum of the C5X and C6X in-plane bends, "active" is the sum of the C5C6 stretch and C5X and C6X bending coordinates, "ring def." is the ring deformation, and "C4O10 str." is the C4O10 stretch.

A similar effect is observed in the methylated uracils; the presence of a single methyl group increases the reorganization energy along the C5C6 stretch from 6% in uracil to 24% and 26% in 5-MeU (T) [13] and 6-MeU [13], respectively, but the presence of a second methyl group does not lead to any significant increase in the reorganization energy along this internal coordinate (25% in 5,6-Me_2U) [14]. Again, the reorganization energy along the C5C6 stretch in doubly methylated

uracil is the average percentage reorganization energy of the singly methylated uracil derivatives.

The C5X and C6X bends are another photochemically active internal coordinate. A significant decrease is expected in the reorganization energy of the C5X or C6X bends when X≠H due to the heavier mass of the substituent compared to H. It is observed that the reorganization energy along the C5X bend in uracil reduces from 13% to 2% in 5-*d*-U. Similarly, the reorganization energy along the C6X bend in uracil reduces from 9% to 3% in 6-*d*-U. With deuteriums on both C5 and C6, the reorganization energies along both the C5X and C6X bends reduces more considerably from 13% and 9% in uracil to 6% and 2% in 5,6-d_2-U, respectively. These decreases appear along the C5 + C6 bends sum, in which the reorganization energy is reduced from 22% in uracil to 18% and 16% in 5-*d*-U and 6-*d*-U and to 8% in 5,6-d_2-U. These results seem to be due to the presence of the heavier mass on the respective site [10-14].

A similar behavior is expected along the C5X and C6X in-plane bending coordinate in the methylated uracil derivatives. The 13% reorganization energy along the C5X bend in uracil decreases to 8% in 5-MeU and the 9% reorganization energy along the C6X bend in uracil decreases to 3% in 6-MeU. Similar to 5,6-d_2-U, the reorganization energy along the C5 + C6 bends sum is reduced from 22% in uracil to 13% in 5,6-Me_2U. However, less of a decrease along the C5 + C6 bends sum is observed in the C5-substituted derivatives – 18% for 5-*d*-U and 23% for 5-MeU [13] - compared to the C6-substituted uracil derivatives, 16% for 6-*d*-U and 10% for 6-MeU. All these results confirm the greater significance of the C5 position in increasing the initial excited-state structural dynamics along the C5 and C6 in-plane bending coordinates.

Comparison of the sum of the reorganization energies of C5C6 stretch and C5 + C6 bends sum (represented as “active” in Table 3) in all the deuterated and methylated uracil derivatives indicates

that the highest reorganization energies along these photochemical active internal coordinates belong to the C5 substituted uracil derivatives (34% and 47% in 5-*d*-U and 5-MeU(T), respectively) in their respective series. This result confirms the significance of C5 in the initial excited-state structural dynamics of these internal coordinates. Also, the reorganization energies of the methylated uracil derivatives are higher than those of the deuterated uracil derivatives, primarily due to the increase in the C5C6 stretching reorganization energy. This result indicates that the initial excited-state distortion seems to be larger when a methyl group is attached to the C5C6 double bond.

The higher reorganization energies of C4O10 stretch coordinates in uracil and all the deuterated derivatives (~ 20%) clearly indicate their resemblance to uracil in the initial excited-state dynamics, which is also obvious on the spectra (1660 cm^{-1}). Considering the relative high reorganization energy along the C5C6 stretch in all the methylated derivatives (< 20%), we propose that the methyl group on C5 or C6 channels the reorganization energy from the C4O10 stretch to the C5C6 stretch, a more photochemically active internal coordinate, and is one of the factors which then dictates the photoproduct differences between uracil and thymine.

The interesting comparison is between the dideutero and dimethyl analogues of uracil. While 5,6-Me_2U demonstrates behavior intermediate between that of 5-MeU and 6-MeU in the C5C6 stretch, in-plane bend and photochemically active internal coordinates [14], 5,6-d_2-U demonstrates *cumulative* effects of the deuterium substitution in the in-plane bend and photochemically active internal coordinate. Like 5,6-Me_2U, the dideutero substitution leads to an intermediate effect on the C5C6 stretch between that of 5-*d*-U and 6-*d*-U. This effect on the initial excited-state structural dynamics of 5,6-d_2-U was difficult to predict. Although both 5-*d*-U and 6-

d-U show reductions in the individual in-plane bend reorganization energy of the substituted carbon, 5,6-Me_2U shows an intermediate behavior in the bend reorganization energy. The result presented here demonstrates that the deuterium-induced reduction in in-plane bend reorganization energies is the dominant effect in determining the initial excited-state structural dynamics.

From these results, a model for the different photochemistry in uracil and thymine emerges. In forming the photochemical products, uracil and thymine both undergo bond lengthening at C5C6 and pyramidalization of the C5 and C6 carbons. In uracil, the excited-state structural dynamics are dominated by the C5 and C6 in-plane bends, as well as the C4O10 stretch. While the role of the C4O10 stretch in uracil's photochemistry is not currently understood, since this bond is unaffected in all photochemical products of uracil, the C5 and C6 in-plane bends may reflect the formation of the zwitterionic state that has been implicated in the pyrimidine photohydrate formation [30]. Ideally, we would be able to observe the out-of-plane bends, as these internal coordinates may be more diagnostic for pyramidalization motions of the C5 and C6 carbons. Unfortunately, these motions are not resonance Raman active in the C_s symmetry of the pyrimidine ring, and not observed in the spectra.

In thymine, however, the initial excited-state structural dynamics are dominated by distortion along the C5C6 stretch and equivalent distortions along the C5 and C6 in-plane bends. These distortions may prime the transition state for formation of the CPD, which time-resolved infrared spectroscopy has shown [31] to occur within the extremely short electronic lifetime of thymine (540 fs) along an essentially barrierless trajectory [31,32]. Within this timeframe, there is very little time to undergo significant additional structural dynamics other than those probed in the Franck-Condon region. More probing of the excited-state structural dynamics, both along the

C4O10 stretching coordinate and at timescales intermediate to those in this study (~10-30 fs) and the previously reported time-resolved infrared study (~100-1000 fs) are required to more fully describe the photochemical pathways in uracil and thymine.

Conclusion

We have compared the initial excited-state structural dynamics of C5 and C6 uracil derivatives derived from the absorption and UV resonance Raman spectra. The substituent rearrangement alters the normal modes, their frequencies, their excited-state slopes and the resulting initial excited-state structural dynamics. By calculating the reorganization energies on an internal coordinate basis, a clearer understanding emerges of the role of the C5 and C6 substituents on the initial excited-state structural dynamics and the resulting photochemistry. The higher sensitivity of the initial excited-state structural dynamics to methyl substituents and to substituents at the C5 position is demonstrated. In addition, deuterium substitution leads to a cumulative reduction on the initial excited-state structural dynamics, compared to an intermediate effect for methyl substitution. This dependence leads to a clear dynamics of in-plane bending and carbonyl distortion for uracil, but in-plane bending and C5C6 double bond distortion for thymine.

Corresponding Author

* Email: Glen R.Loppnow. glen.loppnow@ualberta.ca

Acknowledgements

The authors wish to thank the Natural Science and Engineering Research Council (NSERC) of Canada for partial support of this project through its Discovery Grants and Equipment Grants

programmes.

References

[1] K. H. Kraemer, *Proc. Natl. Acad. Sci. USA* **1997,** *94*, 11-14.

[2] D. G. E. Lemaire, B. P. Ruzsicska, in *Organic Photochemistry and Photobiology*. (Eds.: W. M. Horspool, P.-S. Song), CRC Press, New York, **1995**, pp 1295-1329.

[3] T. Gustavsson, N. Sarkar, E. Lazzarotto, D. Markovitsi, R. Improta, *Chem. Phys. Lett.* **2006,** *429*, 551-557.

[4] T. Gustavsson, A. Banyasz, E. Lazzarotto, D. Markovitsi, G. Scalmani, M. J. Frisch, V. Barone, R. Improta, *J. Am. Chem. Soc.* **2006,** *128*, 607-619.

[5] T. Gustavsson, *J. Phys. Chem. Lett.,* **2010**, *1*, 2025-2030.

[6] P. M. Hare, C. E. Crespo-Hernandez, B. Kohler, *Proc. Natl. Acad. Sci. USA* **2007,** *104*, 435-440.

[7] B. Cohen, P. M. Hare, B. Kohler, B. *J. Am. Chem. Soc.* **2003,** *125* , 13594-13601.

[8] B. Cohen, C. E. Crespo-Hernandez, B. Kohler, *Faraday Discuss.* **2004,** *127*, 137-147.

[9] C. E. Crespo-Hernandez, B. Cohen, P. M. Hare, B. Kohler, *Chem. Rev.* **2004,** *104*, 1977-2019.

[10] S. Yarasi, P.Brost, G. R. Loppnow, *J. Phys. Chem. A* **2007,** *111,* 5130-5135.

[11] S. Yarasi, S. Ng, G. R. Loppnow, *J. Phys. Chem. B* **2009,** *113*, 14336-14342.

[12] S. S. Ng, F. Teimoory, G. R. Loppnow, *J. Phys. Chem. Lett.* **2011**, *2*, 2362-2365.

[13] F. Teimoory, G. R. Loppnow, *J. Phys. Chem. A* **2014**, *118*, 12161-12167.

[14] S. Sasidharanpillai, G. R. Loppnow, *J. Phys. Chem. A* **2014,** *118*, 4680-4687.

[15] E. Fraga, M. A. Webb, G. R. Loppnow, *J. Phys. Chem.* **1996,** *100*, 3278-3287.

[16] M. A. Webb, C. M. Kwong, G. R. Loppnow, *J. Phys. Chem. B* **1997,** *101*, 5062-5069.

[17] A. B. Myers, R. A. Mathies, in *Biological applications of Raman spectroscopy, Vol. 2* (Ed: T. G. Spiro) Wiley-Interscience, New York, **1987**, pp 1-58.

[18] S. Y. Lee, E. J. Heller, *J. Chem. Phys.* **1979,** *71*, 4777-4788.

[19] A. B. Myers, in *Laser Techniques in Chemistry*, Wiley, New York, **1995**; pp 325-384.

[20] A. M. Kelley, *J. Phys. Chem. A* **1999,** *103*, 6891-6903.

[21] B. E. Billinghurst, G. R. Loppnow, *J. Phys. Chem. A* **2006,** *110*, 2353-2359.

[22] B. E. Billinghurst, R. Yeung, G. R. Loppnow, *J. Phys. Chem. A* **2006,** *110*, 6185-6191.

[23] M. J. Frisch, G. W. Trucks, H. B. Schlegel, G. E. Scuseria, M. A. Robb, J. R. Cheeseman, G. Scalmani, V. Barone, B. Mennucci, G. A. Petersson, H. Nakatsuji, M. Caricato, X. Li, H. P. Hratchian, A. F. Izmaylov, J. Bloino, G. Zheng, J. L. Sonnenberg, M. Hada, M. Ehara, K. Toyota, R. Fukuda, J. Hasegawa, M. Ishida, T. Nakajima, Y. Honda, O. Kitao, H. Nakai, T. Vreven, J. A. Montgomery, Jr., J. E. Peralta, F. Ogliaro, M. Bearpark, J. J. Heyd, E. Brothers, K. N. Kudin, V. N. Staroverov, R. Kobayashi, J. Normand, K. Raghavachari, A. Rendell, J. C. Burant, S. S. Iyengar, J. Tomasi, M. Cossi, N. Rega, J. M. Millam, M. Klene, J. E. Knox, J. B. Cross, V. Bakken, C. Adamo, J. Jaramillo, R. Gomperts, R. E. Stratmann, O. Yazyev, A. J. Austin, R. Cammi, C. Pomelli, J. W. Ochterski, R. L. Martin, K. Morokuma, V. G. Zakrzewski, G. A. Voth, P. Salvador, J. J. Dannenberg, S. Dapprich, A. D. Daniels, Ö. Farkas, J. B. Foresman, J. V. Ortiz, J. Cioslowski, and D. J. Fox, Gaussian, Inc., Wallingford CT, **2009**

[24] J. S. Singh, *Spectrochim. Acta.* **2015**, *137A*, 625-640.

[25] L. S. Khaikin, O. E. Grikina, N. Vogt, N. F. Stepanov, *Russ. J. Phys. Chem. A* **2012**, *86*, 1855-1861.

[26] J. M. L. Martin, C. Van Alsenoy, *GAR2PED*. University of Antwerp: Antwerp: The Netherlands, 1995.

[27] S. L. Zhang, K. H. Michaelian, G. R. Loppnow, *J. Phys. Chem. A* **1998**, *102*, 461-470.

[28] S. Yarasi, G. R. Loppnow, *J. Raman Spectrosc.* **2007**, *38*, 1117-1126.

[29] R. A. Marcus, *Rev. Mod. Phys.* **1993,** *65*, 599-610.

[30] D. M. Hovorun, I. V. Kondratyuk, *Biopolim. Kletka* **1996**, *12*, 42-48.

[31] W. J. Schreier, T. E. Schrader, F. O. Koller, P. Gilch, C. E. Crespo-Hernandez, V. N. Swaminathan, T. Carell, W. Zinth, B. Kohler, *Science* **2007**, *315*, 625-629.

[32] J. M. L. Pecourt, J. Peon, B. Kohler, *J. Am. Chem. Soc.* **2001**, *123*, 10370-10378.